ELSEVIER

Materials Science and Engineering B 131 (2006) 281–284

MATERIALS SCIENCE & ENGINEERING B

www.elsevier.com/locate/mseb

Short communication

# Nanomechanical characteristics of $Ba_xSr_{1-x}TiO_3$ thin films

Sheng-Rui Jian [a], Win-Jin Chang [b,*], Te-Hua Fang [c], Liang-Wen Ji [d], Yu-Jen Hsiao [e], Yee-Shin Chang [d]

[a] *Department of Electrophysics, National Chiao Tung University, Hsinchu 300, Taiwan*
[b] *Department of Mechanical Engineering, Kun Shan University, Tainan 710, Taiwan*
[c] *Institute of Mechanical and Electromechanical Engineering, National Formosa University, Yunlin 632, Taiwan*
[d] *Department of Electro-Optics Engineering, National Formosa University, Yunlin 632, Taiwan*
[e] *Department of Materials Science and Engineering, National Cheng Kung University, Tainan 701, Taiwan*

Received 29 December 2005; received in revised form 7 March 2006; accepted 18 March 2006

**Abstract**

The nanomechanical properties of barium strontium titanate ($Ba_xSr_{1-x}TiO_3$, $x = 0$–1) deposited on a silicon substrate were investigated using the metalorganic deposition method. The characteristics of the $Ba_xSr_{1-x}TiO_3$ thin film's crystalline structure and surface roughness were achieved by means of X-ray diffraction (XRD) and atomic force microscopy (AFM). The results indicated that as the Ba content was decreased and therefore the Sr content was increased a lower leakage current density and a smaller grain size were obtained. Also the mechanical properties such as hardness, Young's modulus and contact stress–strain were also studied by nanoindentation.


*Keywords:* BST; XRD; AFM

Perovskite ferroelectric thin films, barium strontium titanate ($Ba_xSr_{1-x}TiO_3$, BST) have been of great interest for their use in dynamic random access memories (DRAM), tunable microwave devices, infrared sensors and electro-optical devices [1–5]. BST thin films' electrical and optical properties, such as, high dielectric constant, large electro-optical coefficient and low optical losses are critical for these applications [6–8].

Despite extensive investigations of several different properties of BST thin films, there is still lacking sufficient research systematically correlating the mechanical and structural relationships on a nanometer-scale for designing advanced optoelectronic devices. It is essential that studies continue on the mechanical characterization of these thin films to recognize how the relative parameters, such as Ba content, affect the material structures and the properties for use in advanced applications.

Modern nanoindentation testing equipment allows penetration depth curves to be measured as a function of load where the loads extend down to the range of micro-Newtons, resulting in typical penetration depths in the range of nanometers. This technique is well suited for examining the mechanical properties of thin films [9,10].

In the research presented here, the microstructure and mechanical properties of $Ba_xSr_{1-x}TiO_3$ thin films of different Ba/Sr composition ratios, produced by use of the metalorganic decomposition (MOD) method, have been studied.

In this study, barium acetate $Ba(CH_3COO)_2$, strontium acetate $Sr(CH_3COO)_2$ and Ti-isopropoxide $Ti(OC_3H_7)_4$ were used as the starting materials. An optimum ratio of acetic acid and ethylene glycol, $R_{ac/eg} = 3{:}1$, was selected as the solvent. Fomamide was selected as an additive to adjust the solution's viscosity in order to reduce the cracks in the deposited BST thin films. Barium acetate and strontium acetate with a molar ratio of $x{:}1-x$ ($x = 0$–1) was completely dissolved into heated glacial acetic acid and then ethylene glycol was

* Corresponding author.
*E-mail address:* changwj@mail.ksu.edu.tw (W.-J. Chang).

0921-5107/$ – see front matter © 2006 Elsevier B.V. All rights reserved.
doi:10.1016/j.mseb.2006.03.025

added to the solution which caused a condensation reaction between the glacial acetic acid and the ethylene glycol. Then Ti-isopropoxide was added to the solution, after that formamide was added to adjust the viscosity of the BST precursor solution.

The $Ba_xSr_{1-x}TiO_3$ precursor solution was spin-coated on the silicon substrates at a speed of 4000 rev/min for 30 s. The substrates used were p-type silicon (1 0 0). After the spin coating was completed, the samples were heated from 25 to 150 °C for 10 min to dry the gel and then pyrolyzed at 400 °C for 30 min. The crystallization was carried out by a in a horizontal batch type furnace annealing process in atmosphere ambiance. The specimens were annealed at 600 °C for 40 min to cause the film to crystallize into the perovskite phase. BST thin films with a desired thickness of 200 nm were obtained.

The crystal structure of the BST thin films was analyzed by X-ray diffractometry (XRD) on a SIEMENS D5000 diffractometer using Cu Kα (λ = 1.5418 Å) radiation. The surface morphology was analyzed by atomic force microscopy (TM/Veeco CP-R SPM, USA). Nanomechanical properties of BST thin films were determined using a Nanoindenter (Hysitron Triboscope, USA) with a three-sided pyramidal Berkovich indenter tip for all indentation testing, performed at room temperature. For each specimen, a maximum indentation load of 50 μN and a loading time of 10 s were used. Hardness and elastic modulus were determined by means the method of Oliver and Pharr [11], and the Poisson's ratio of thin films was assumed to be 0.3 for calculating the thin film's Young's modulus.

XRD measurements of five uniform composition thin films are shown in Fig. 1, it indicates a pseudo-cubic, or perovskite phase without preferred orientation. In other word, the results show that there is no intermediate phase and the BST thin films where well crystallized when annealed at 600 °C for 40 min. For further discussion, the (1 1 0) peaks from the five samples were chosen to investigate the crystalline phase evolution and

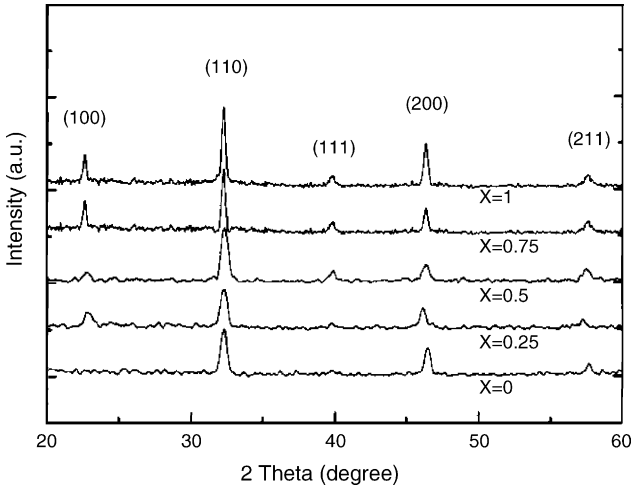


Fig. 1. XRD patterns of $Ba_xSr_{1-x}TiO_3$, ($x$ = 0–1) (the reflections are marked by their indices).

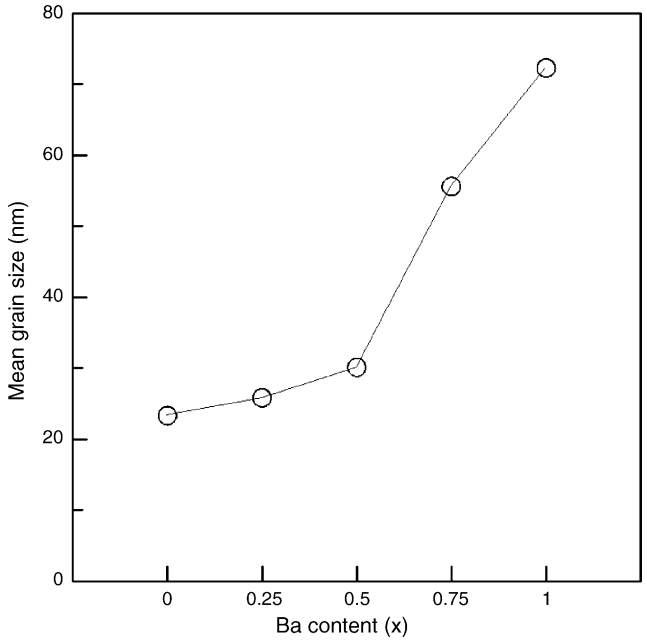


Fig. 2. The BST thin film mean grain size as a function of Ba content.

centered at $2\theta \approx 32.54°$ (other peaks were shown in Fig. 1). Moreover, we found that the BST film with high Ba content had better polycrystalline quality, as indicated from its XRD spectra.

The grain size of the films was calculated by using the full width at half maximum (FWHM) of the dominant (1 1 0) peak by Scherrer's formula [12]. As seen in Fig. 2 mean grain size of the BST thin films ranged from 23.31 to 72.27 nm and the grain size decreased as the Ba content was decreased.

The surface morphology of the BST films within a scan area of 1 μm × 1 μm was measured by AFM as shown in Fig. 3. It can be clearly seen that the dominant feature of the films is the appearance of small isolated islands. The average roughness ($R_a$) and root-mean-square (R.M.S.) of the BST thin films at different Ba/Sr ratio are shown in Fig. 4. The values of average surface roughness of the $Ba_{0.25}Sr_{0.75}TiO_3$, $Ba_{0.5}Sr_{0.5}TiO_3$ and $Ba_{0.75}Sr_{0.25}TiO_3$ thin films were 0.22 nm, 0.16 and 0.34 nm, respectively. It was found that the best, smoothest surface was obtained when the Ba/Sr ratio was 0.5. The average surface roughness values of the $BaTiO_3$ and $SrTiO_3$ thin films were 0.15 and 0.34 nm, respectively.

Fig. 5 shows the indentation load-penetration depth curves of the BST thin films. To avoid the influence of the substrate on the mechanical properties of thin films, the nanoindentation depths of thin films were kept to less than 10% of films thickness. Further information can be found in the study performed by Oliver and Pharr [11]. The hardness and elastic modulus of the BST thin films are shown in Fig. 6. It was found that both the hardness and Young's modulus of the $Ba_xSr_{1-x}TiO_3$ thin films decreased as the Ba ratio was increased from 0.25 to 0.75. The hardness and Young's modulus values ranged from 1.63 to 1.41 GPa and from 75.9 to 59.4 GPa, respectively.

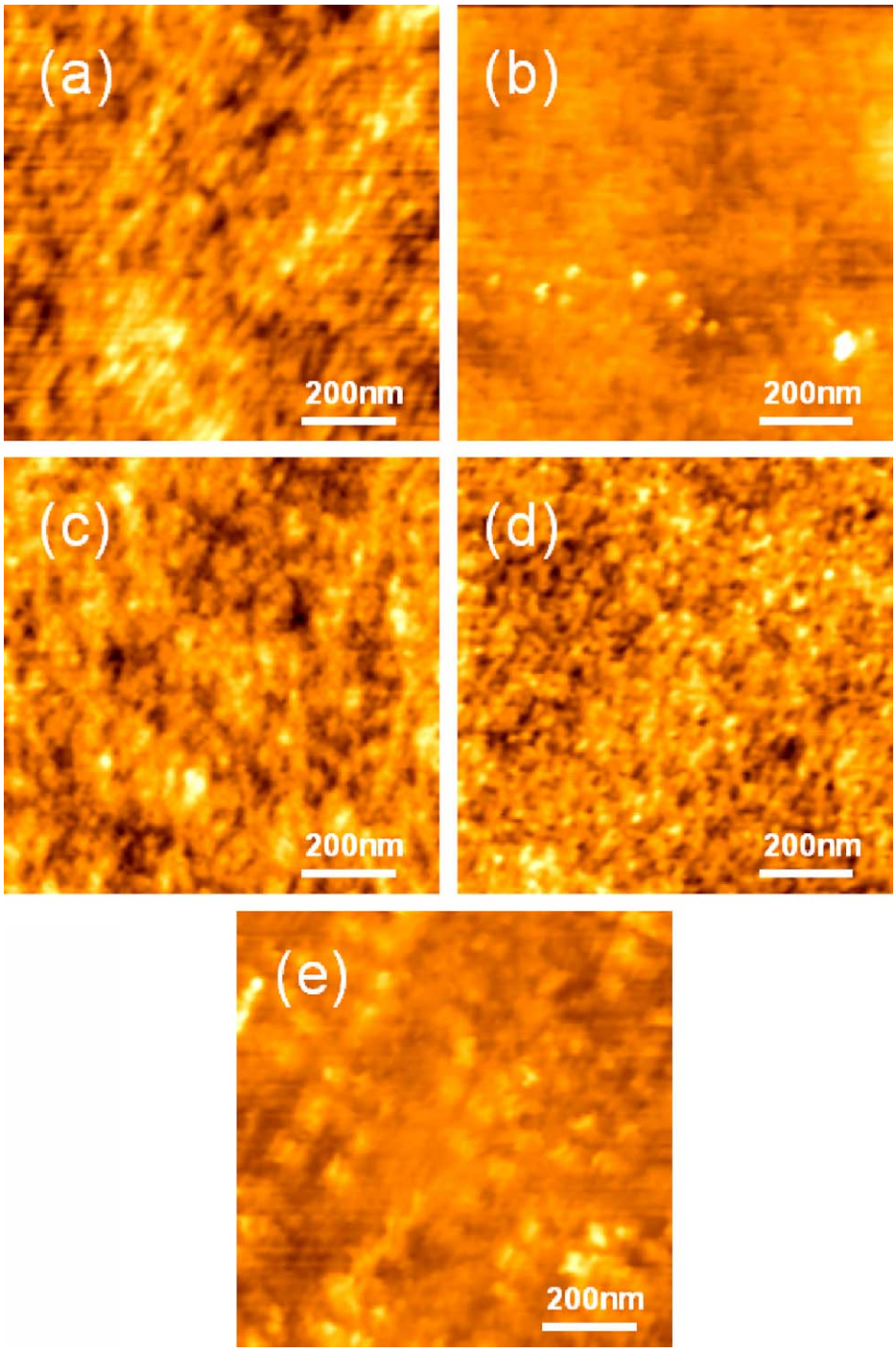


Fig. 3. AFM images of $Ba_xSr_{1-x}TiO_3$ ($x = 0$–1): (a) $BaTiO_3$, (b) $Ba_{0.75}Sr_{0.25}TiO_3$, (c) $Ba_{0.5}Sr_{0.5}TiO_3$, (d) $Ba_{0.25}Sr_{0.75}TiO_3$ and (e) $SrTiO_3$.

The contact stress–strain relationship of the different BST thin films is shown in Fig. 7. Using contact stress–strain analysis, it is to better understand the mechanisms of plastic deformation. The $Ba_{0.5}Sr_{0.5}TiO_3$ film was able to bear the largest stress of 27.32 GPa under a contact strain of less than 0.36 and had the best contact stress–strain relationship.

In summary, the microstructure, surface morphology and nanomechanical characterizations of the $Ba_xSr_{1-x}TiO_3$ thin films deposited using different Ba/Sr ratios were investigated. All of the films showed a (1 1 0)-oriented perovskite phase. The nanoindentation results showed that the hardness and Young's modulus both decreased as the Ba ration was increased from 0.25 to 0.75. The contact stress–strain relationship indicates that

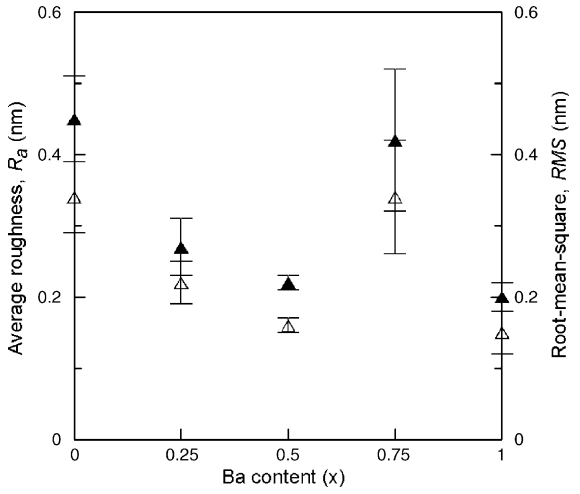


Fig. 4. Surface roughness, $R_a$ (△) and R.M.S. (▲), as a function of Ba content for BST thin films.

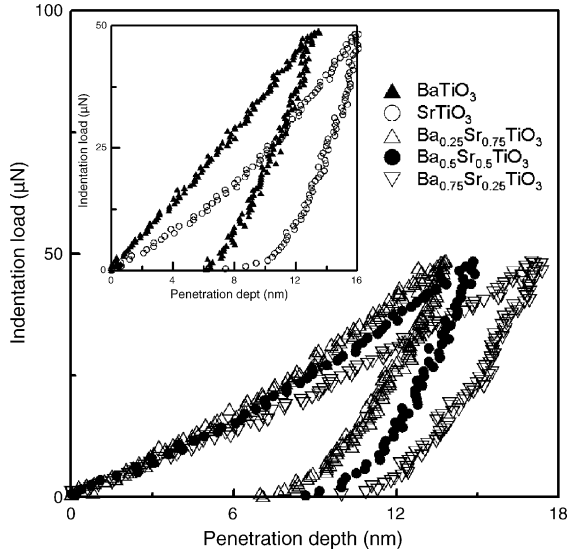


Fig. 5. Load-penetration depth curves for BST thin films at a maximum load of 50 μN.

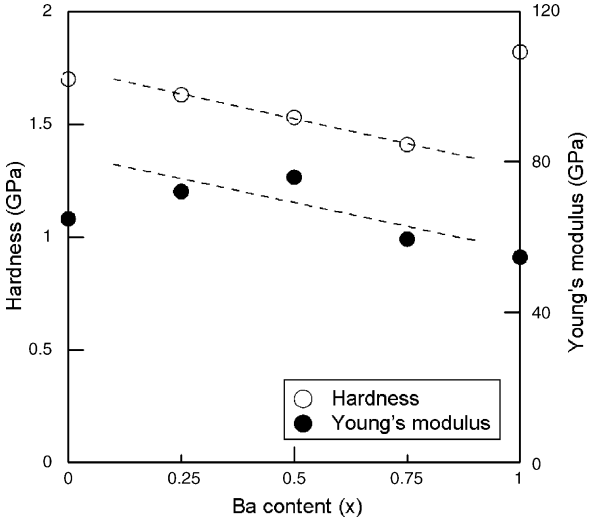


Fig. 6. Hardness and Young's modulus of BST thin films measured as a function of Ba content.

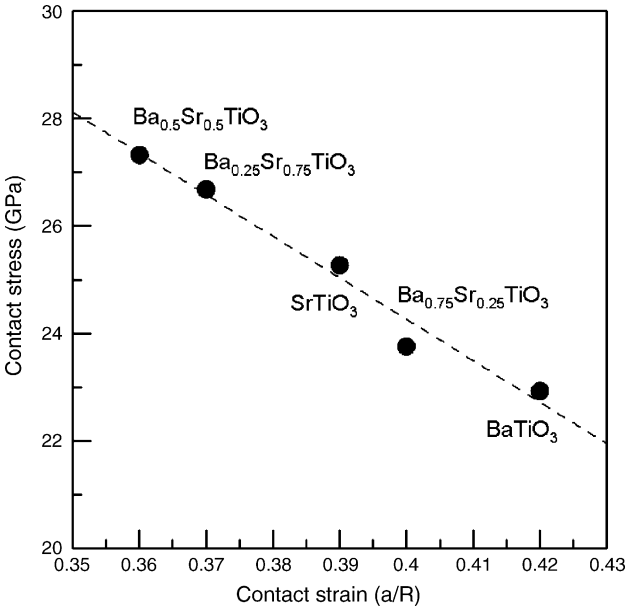


Fig. 7. Contact stress–strain relationship of BST thin films.

$Ba_{0.5}Sr_{0.5}TiO_3$ film can bear a larger amount of stress and have a lower surface strain.

## Acknowledgement

This work was partially supported by the National Science Council of Taiwan, under Grant Nos. NSC 94-2218-E-150-045 and NSC 94-2212-E-168-004.

## References

[1] A.I. Kingon, J.P. Maria, S.K. Streiffer, Nature 406 (2000) 1032.
[2] N.A. Pertsev, V.G. Koukhar, R. Waser, S. Hoffmann, Appl. Phys. Lett. 77 (2000) 2596.
[3] C. Basceri, S.K. Streiffer, A.I. Kingon, R. Waser, J. Appl. Phys. 82 (1997) 2497.
[4] E. Ngo, P.C. Joshi, M.W. Cole, C.W. Hubbard, Appl. Phys. Lett. 79 (2001) 248.
[5] Y.H. Xu, J.D. Mackenzie, Integr. Ferroelectr. 1 (1992) 17.
[6] O. Auciello, J.F. Scott, R. Ramesh, Phys. Today 51 (1999) 22.
[7] K. Abe, S. Komatsu, Jpn. J. Appl. Phys. 32 (1993) 4186.
[8] M.N. Kamalasanan, S. Chandra, Appl. Phys. Lett. 59 (1991) 3547.
[9] T.H. Fang, W.J. Chang, Microelectron. Eng. 65 (2003) 231.
[10] T.H. Fang, S.R. Jian, D.S. Chuu, J. Phys. D: Appl. Phys. 36 (2003) 878.
[11] W.C. Oliver, G.M. Pharr, J. Mater. Res. 7 (1992) 1564.
[12] B.D. Cullity, Elements of X-Ray Diffraction, Addison-Wesley, Reading, MA, 1978.